

# The QCD Spectrum

Chris Michael<sup>a</sup> \*

<sup>a</sup>D. A. M. T. P., University of Liverpool,  
Liverpool L69 3BX, U.K.

Recent results in light hadron spectroscopy are reviewed. Attention is given to the requirements of precision determinations in lattice gauge theory. Different methods for extracting the running coupling constant  $\alpha_S$  are compared. Some recent results in determining the nature of the interaction between static quarks are also discussed.

## 1. INTRODUCTION

In principle lattice Monte Carlo methods are capable of precision evaluations of the QCD spectrum. Furthermore one can study the effect of varying the fundamental parameters, namely the quark masses, from their experimental values.

In order to organise the discussion, I present the current state of QCD spectrum calculations by comparing them to the ideal target of perfect accuracy. The topics to be covered are the control of the discretisation errors, finite volume errors, quark mass errors and ground state extraction errors.

In a later section I discuss the link to perturbation theory. This is relevant for an accurate extraction of the running coupling of QCD. It is also relevant for other perturbative contributions, such as the matching coefficients ( $Z$ ) needed to relate lattice matrix elements to continuum matrix elements.

The interaction between static colour sources is discussed since recent results shed light on the confinement mechanism.

## 2. PRECISION QCD ON A LATTICE

One aim of lattice QCD is to be able to reproduce accurately the hadron spectrum. This will then give confidence in the method and will allow evaluations of new quantities of interest such as matrix elements. A study of the effect of varying

the quark masses is also of great interest. Because of the extreme computational resource needed for full QCD simulation, progress can be made by studying quenched and partially quenched systems as well.

There have been new dynamical fermion calculations reported [1,2] this year. A growing trend is to compromise between quenched and dynamical calculations by using partial quenching. This implies using valence quarks with different properties (mass, or discretisation) from the dynamical (sea) quarks present in the vacuum. The quenched approximation itself is still a rich subject of study and much remains to be done.

The ultimate aim of lattice QCD calculations is to extract physical results applicable to the continuum limit. To organise the presentation of the current state of the subject, I consider in turn the various approximations inherent in the lattice approach.

### 2.1. Discretisation Errors

The lattice spacing  $a$  is introduced to regulate the field theory of QCD. Then dimensionless ratios of mass values determined from lattice calculations will have errors of order  $Ma$  or  $\Lambda a$ , in general, where  $M$  is a mass value and  $\Lambda$  represents a typical QCD momentum scale. The continuum limit is obtained by extrapolating such ratios to  $a = 0$ . Even if only states with light quarks (u,d and s) are studied, the masses can be large: the  $\Omega^-$  has a mass of 1.67 GeV. So, a priori, corrections of order  $Ma$  can be large for current values of the lattice spacing of  $a^{-1} \leq 3$  GeV.

\*To be published in the Proceedings of Lattice 1994, Nucl. Phys B (Proc. Suppl.), Liverpool Preprint LTH 340, hep-lat/9412032, December 5, 1994

Note that dimensionless ratios such as  $M/\Lambda$  will have discretisation errors of order  $g^2$  or  $\log(a)$  since  $\Lambda$  is defined through matching with perturbation theory. Thus one should not use such ratios to obtain a continuum limit.

For the study of hadrons made of quarks, the Wilson discretisation of fermions is simple and flexible. It has errors of  $\mathcal{O}(a)$ . As an illustration, consider the nucleon to  $\rho$  mass ratio. The most extensive results have been obtained in the quenched approximation. Then keeping the lattice volume constant in physical units (at  $M_\rho L \approx 9$ ), and after extrapolating the quark masses to the physical light quark masses, the ratio has been fitted [3] as

$$\frac{M_N}{M_\rho} = 1.28(7) + 0.27M_\rho a \quad (1)$$

as illustrated in fig 1. This rate of  $a$ -dependence implies that an extrapolation in  $a$  is needed even with data at  $\beta = 6.17$  on  $32^2 \times 30 \times 40$  lattices where  $M_\rho a \approx 0.3$ . The results shown in fig. 1 from the GF11 group [3] are the most comprehensive available. Nevertheless, the statistical errors are quite large so that, even in the quenched approximation, results for  $M_N/M_\rho$  are not yet precise. Thus although the GF11 data are consistent after extrapolation in  $a$  and  $L$  with the experimental ratio of 1.22, much work still needs to be done to get an accurate calibration of the quenched approximation value. A recent analysis by the LANL group [4] using  $32^3 \times 64$  lattices at  $\beta = 6.0$  has also produced relevant data and this is shown in fig 1. Even with 80 configurations, they are unable to reduce their errors sufficiently to provide a stringent cross check.

The situation for staggered fermion discretisation in the quenched approximation is summarised in the review by Gottlieb [5]. Again current data are consistent with an  $a$ -dependence which yields a continuum limit close to the experimental ratio of 1.22.

Given the substantial  $\mathcal{O}(a)$  corrections observed with Wilson fermions, much effort has gone into formulations that improve the discretisation errors. The SW-Clover fermionic action has  $\mathcal{O}(\alpha_S a)$  errors with a correct treatment of observables [6]. Simulations using this action [7,8]

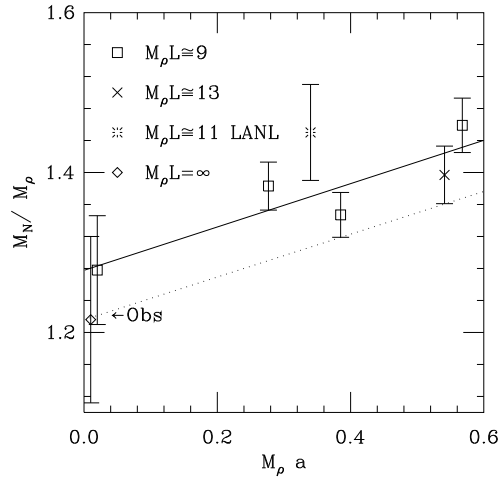


Figure 1. The nucleon to  $\rho$  mass ratio from quenched results [3,4] extrapolated to the chiral limit.

at  $\beta = 6.0$  and  $6.2$  are not yet of sufficiently high statistics to enable  $M_N/M_\rho$  to be determined accurately. In fact I return to discuss the current state of the UKQCD nucleon data when I discuss ground state extraction later.

For heavy quarks, the hadron spectrum is even heavier and  $\mathcal{O}(Ma)$  corrections are even more important. For c quarks, the SW-clover formulation is promising and has been successfully used. For b quarks, it is feasible to use a formalism which treats the heavy quark explicitly: non-relativistically (NRQCD), as static quarks, or by a discretisation of heavy quark effective theory. Such heavy quark calculations are covered in talks by Sommer [43], Sloan [10] etc.

Another approach to improving the discretisation errors, is the mean-field improved formalism [11]. This provides an impressive description of many features. What is needed is a method to estimate reliably the residual error.

The goal of removing completely the discretisation errors is achieved by the perfect action. For the gluonic sector of the theory, the standard Wilson plaquette discretisation already has errors only  $\mathcal{O}(a^2)$ . Current approximations to the perfect action are reported by Hasenfratz [12]. As

well as a perfect action, perfect observables will be needed to remove lattice artifacts such as the lack of rotation invariance in the static potential for example.

## 2.2. Finite Volume Errors

Corrections in a spatial volume  $L^3$  can arise because of exchange of the lightest hadron (the  $\pi$  meson of mass  $m_\pi$ ) around the boundary. Finite size corrections can also occur if the radius of a hadronic state  $r_h$  is not small compared to  $L$ . To remove these corrections, one needs

$$m_\pi L \gg 1, \text{ and } r_h/L \ll 1 \quad (2)$$

The finite value of  $L$  also makes momentum discrete and for some studies it is appropriate to require the minimum momentum  $q_{min} = 2\pi/L \ll m_\pi$ .

There can be surprises: in pure gauge studies the finite size effects on the glueball spectrum are significant out to  $m_G L \approx 8$  where  $m_G$  is the lightest state (the  $0^{++}$  glueball). So “ $\gg$ ” really means “ $\gg$ ” not just “ $>$ ” in this case. This is understood and arises since the dominant finite size effect comes from flux loops encircling the spatial boundary (called spatial Polyakov loops or torelons).

Moreover, these effects were predicted [13] to be approximately twice as strong in full dynamical quark simulations since one torelon (rather than two) can then mix with the glueballs.

At the Lattice 1993 conference, results were presented [14] showing that finite size effects on the hadron spectrum indeed appear worse for full QCD compared to the quenched approximation. The origin of the effect can be seen from the example of a meson correlation illustrated in fig 2 where one quark propagator encircles the spatial boundary. So effectively, the quark feels the (non-abelian) phase of the spatial Polyakov loop. Now in the quenched approximation, the  $Z_3$  symmetry ensures that such loops have zero expectation value. In contrast, the quark mass term in the dynamical quark case breaks this  $Z_3$  symmetry. This then allows the Polyakov loops to become non-zero on average and so enhances their contribution to finite size effects.

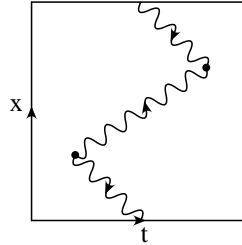


Figure 2. A finite size effect

A new study of this topic was reported by the APE collaboration [2]. They use anti-periodic spatial boundary conditions on the Wilson dynamical (sea) quarks. This ‘polarises’ the Polyakov loops so reducing statistical errors. They then explore the magnitude of the residual finite size effects by measuring  $\pi$  and  $\rho$  meson masses using both periodic and anti-periodic spatial boundary conditions for the valence quarks. With  $L \approx 1.5$  fm, they find finite size effects on the masses of only a few per cent.

## 2.3. Quark mass extrapolation

The requirement is to incorporate fully quarks of physical mass in the QCD vacuum. Because of the large computational resource needed, typical studies are limited to spatial sizes of  $16^3$  and quark masses corresponding to  $m_\pi/m_\rho \approx 0.3$ . For technical reasons, one of the preferred methods is to include two flavours of degenerate light quarks using the staggered fermion discretisation.

In most simulations, the main effect of including dynamical quarks is a shift of the  $\beta$  value. Thus, instead of comparing at the same bare  $\beta$  value, one should compare at the same lattice spacing (ie same  $ma$  value). Then ratios of masses appear very little changed compared to the quenched case. Since the present quenched spectrum is consistent with the experimental data, it is to be expected that adding dynamical quarks will not change this state of affairs. One expected effect of dynamical quarks is to modify the small distance forces. This region is amenable to perturbative evaluation and, because of the factor  $33 - 2N_f$  in the denominator

of the running coupling, a stronger interaction is expected at short distance. This can be tested by looking at the force between static quarks at short distance [15].

An extrapolation of the light quark masses to the physical value is needed. For full QCD, data are not sufficiently precise to explore this extrapolation accurately. Further work is needed to check whether the extrapolation is smooth: some “threshold effect” might occur as the quark mass is reduced (the opening up of the decay  $\rho \rightarrow \pi + \pi$  has been suggested).

For studies of the quenched (and partially-quenched where the valence quarks are different in mass from the dynamical or sea quarks) approximation, the limit of small quark masses is potentially tricky. This has been studied in generalised chiral effective theories and is reported on by Gupta [16]. To circumvent these problems associated with extrapolation to the chiral limit, one way is to present lattice results at the quark mass used. This is appropriate for comparing between lattice calculations (eg. the Edinburgh plot) but may also be used to compare with experiment in principle. From lattice results for hadron masses for a range of quark masses, it should be possible to develop an accurate semi-empirical mass formula relating the hadron mass to the masses of its quark ingredients. Then experimental data for the combinations of quark masses (u, d and s) accessible can be used to fix the coefficients in such a model. Thus lattice data would be used to validate a quark-model mass formula which could then be used for direct comparison with lattice results.

While computational resources limit full QCD work, there is still a lot of physics that can be studied in the quenched approximation. The quenched approximation has spontaneous chiral symmetry breaking and gives a surprisingly good overall description of the QCD spectrum. It is even possible to estimate matrix elements within the quenched approximation which enable one to study processes beyond that approximation. Examples are the decay  $\rho \rightarrow \pi + \pi$ ; glueball decay and the  $\eta'$  mass.

Here I discuss some of these analyses to illustrate the possibilities.

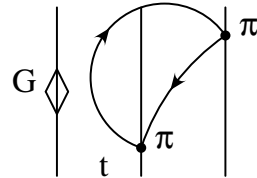


Figure 3. The glueball  $\pi\pi$  correlation

### 2.3.1. Glueball decay

The glueball spectrum has been studied in the quenched approximation [17,18] and the lightest glueball is found to be the  $J^{PC} = 0^{++}$  state at around 1600 MeV with the next heaviest state of  $2^{++}$ .

Within the quenched approximation, the lightest glueballs cannot decay. In full QCD, they can decay to mesons: for instance a pair of pseudoscalar mesons. There will also be mixing between glueballs and mesons with quark content.

There have been 20 years of unsuccessful experimental attempts to identify a glueball. To guide this search, it is important to estimate the magnitude of the matrix elements between glueballs and light quark mesons. Then, should the matrix elements be small, the assignment of glueball status could be made with confidence. Candidates for the  $0^{++}$  glueball are the  $f_0(1590)$  meson with width  $180 \pm 17$  MeV and the  $f_J(1710)$  meson (was called  $\Theta(1690)$ ) which has a decay width of  $140 \pm 12$  MeV.

From the point of view of lattice evaluation, such matrix elements are hard to measure because of a mis-match between the techniques used to extract glueballs and those used for light quark mesons. A clear glueball signal can only be obtained by analysing many configurations (typically thousands of independent configurations with all time-slices used as a source). Because of the computational overhead of inverting the fermionic matrix, quark propagators are usually only evaluated for hundreds of configurations and from only one source per configuration. Furthermore the glueball signal only extends for a few time steps whereas a pseudoscalar meson can be

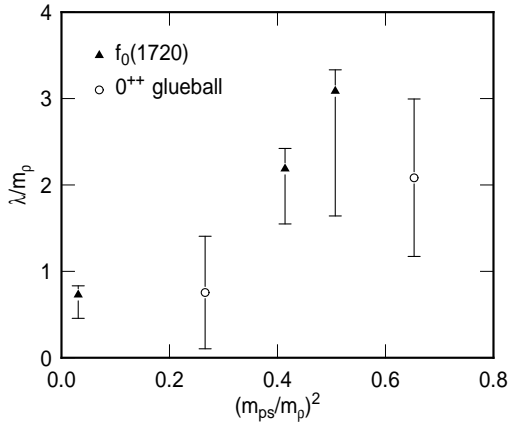


Figure 4. The glueball decay coupling.

followed out to very large time.

A pioneering attempt to tackle this problem has been made by the GF11 group [19]. They use lattices of spatial size  $16^3$  at  $\beta = 5.7$ . Using Wilson quarks with  $K = 0.165$ , they measure 3800 configurations. They are able to isolate the  $0^{++}$  glueball, pion and two pion states. The two pion state is calibrated by exploring expectation values of 4 pion operators. Then the matrix element between a glueball and such a two pion state is studied - see fig 3. In principle the intermediate state has many different contributions: glueball, excited glueballs,  $\pi(k) + \pi(-k)$  with relative momentum  $k = 2\pi n/L$  and  $0^{++}$  mesons. To separate these contributions by studying the  $t$ -dependence of the observable is difficult in principle and hopeless in practice. Since a reasonable signal only survives out to  $t = 1$  with their current statistics, the GF11 group can make, at best, a very rough estimate of the size of the matrix element. Even such a rough estimate can be useful: for example by indicating that a large glueball width is not allowed. In the quenched approximation the glueball does not decay and, moreover, the analysis is performed with a choice of quark mass such that  $m(0^{++}) \approx 2m_\pi$ . Thus the on-shell glueball decay matrix element can be estimated from the lattice measurements.

The result shown in fig 4 is consistent, within

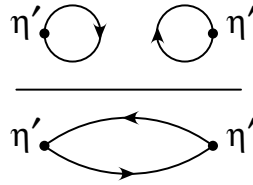


Figure 5. The ratio of disconnected to connected diagrams.

large errors, with that from the observed decay of the  $f_J(1710)$  meson. Some evidence is also obtained that the decay matrix element increases with increasing pseudoscalar mass - as observed experimentally. See ref [19] for more details.

### 2.3.2. The $\eta'$ mass

In the quenched approximation, there are no quark loops in the vacuum. Then, since the vacuum has isospin zero, the flavour octet and singlet pseudoscalar mesons ( $\eta_8$  and  $\eta_1$ ) will be degenerate if all quark masses are the same. Taking the strange quark mass into account from the  $\pi$  and K leads to an  $\eta_8$  at 567 MeV and an  $\eta_1$  at 412 MeV. Experimentally the mixing is such that approximately the  $\eta_8$  is the  $\eta(547)$ , while the  $\eta_1$  is the heavier  $\eta'(958)$  meson. Thus in the quenched approximation, the contribution from the  $\eta'$  will have a mass which is much too low. This, incidentally, is at the root of the modified chiral behaviour in the quenched approximation.

Within the quenched approximation one may study the mixing between quark loops and the  $\eta$  mesons explicitly. Let  $P_8 = (p^2 + m_8^2)^{-1}$  be the quenched  $\eta$  propagator (which is the same as the  $\eta'$  propagator in the quenched approximation), Then consider the effect of a quark loop  $Q$  on the  $\eta'$  propagator  $P_1 = (p^2 + m_1^2)^{-1}$ :

$$\begin{aligned} P_1 &= P_8 - P_8 Q P_8 + P_8 Q P_8 Q P_8 + \dots \\ &= \frac{1}{P_8^{-1} + Q} = \frac{1}{p^2 + m_8^2 + m_0^2} \end{aligned} \quad (3)$$

Thus  $m_1^2 = m_8^2 + m_0^2$  where  $m_0^2$  is the matrix element of a quark loop  $Q$  in the quenched vacuum. This mixing works to increase the mass of the

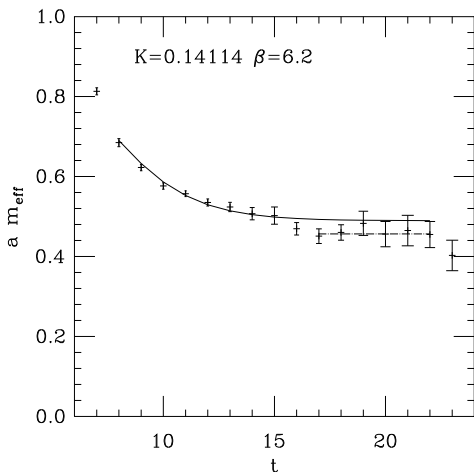


Figure 6. The nucleon effective mass versus  $t$  from UKQCD LL data with one and two exponential fits.

singlet - so giving a chance to obtain the experimental  $\eta' - \eta$  mass splitting. Lattice methods to explore this have been proposed [20]. The basic idea is to compare the disconnected  $\eta'(0)\eta'(t)$  correlator with the connected correlator - see fig 5. The ratio is proportional to the required mixing matrix element  $m_0^2$ . The technical difficulty is to measure the disconnected correlator: an ingenious method was used to cut down the number of propagator inversions by putting sources at each spatial site on a timeslice and allowing gauge invariance to select the required contribution. An analysis using Wilson valence quarks at  $\beta = 5.7$  on  $12^3 20$  and  $16^3 20$  lattices yields mixing  $m_0 = 751 \pm 30$  MeV to be compared to the experimental value

$$m_0^2 = m_{\eta'}^2 - m_8^2 \approx (852 \text{ MeV})^2 \quad (4)$$

So indeed quenched QCD does yield a reasonable understanding of the  $\eta'$  mass.

The Witten-Veneziano formula relates the  $\eta$  mass mixing to the topological susceptibility  $\chi$  by

$$m_0^2 = \frac{2N_f \chi}{f_\pi^2} \quad (5)$$

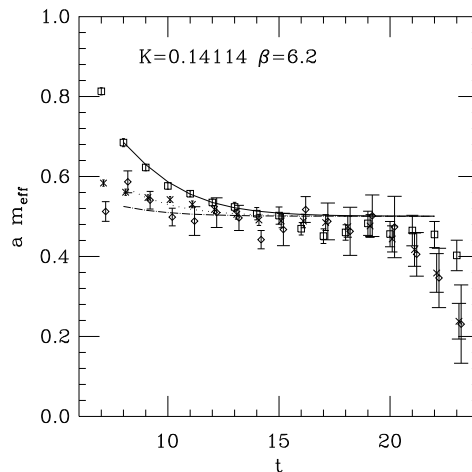


Figure 7. The nucleon effective mass versus  $t$  from UKQCD preliminary data for LL(squares), SL(crosses) and SS(diamonds) with a two exponential fit.

Measurements of the topological susceptibility in lattice gauge theory are plagued with uncertainties from lattice artifacts. Using the cooling method on the same lattices as above, a result of  $m_0^2 = (1146 \pm 67 \text{ MeV})^2$  was obtained [20]. This is qualitatively similar to the value obtained by studying the mixing directly and is further confirmation that the underlying physics of the  $\eta'$  is understood.

#### 2.4. Ground state extraction

The euclidean time formulation implies that eigenstates of the transfer matrix contribute to hadronic correlators  $\langle H^a(0)H^b(t) \rangle$  as

$$\begin{aligned} C_{ab}(t) &= \langle H^a(0)H^b(t) \rangle \\ &= h_0^a h_0^b (e^{-m_0 t} + e^{-m_0(L-t)}) + \\ &\quad h_1^a h_1^b (e^{-m_1 t} + e^{-m_1(L-t)}) + \dots \end{aligned} \quad (6)$$

where  $h_i^c$  is the amplitude to produce eigenstate  $i$  from operator  $H^c$ . The expression is written assuming periodic boundary conditions in time for bosonic eigenstates. The data is usually presented by computing an effective mass from  $m_{\text{eff}}(t) = -\log(C(t)/C(t-1))$ . The ground state contribution dominates  $m_{\text{eff}}(t)$  at large  $t$  since

$m_0 < m_i$  for all  $i \neq 0$ . In practice, extracting the ground state mass  $m_0$  from data with statistical errors which increase with  $t$  is subtle. I wish to emphasize that a good procedure is:

- (i) a multi-exponential fit to the widest acceptable  $t$ -range with
- (ii) several hadronic operators  $H^a$  to stabilise the fit.

One way to understand this guide is that the ground state is only determined accurately when an estimate of the first excited state is available. This is necessary since the energy difference controls the rate of approach of  $C_{ab}(t)$  to the expression given by the ground state component alone. However, fitting 2 (or more) exponentials to just one function  $C(t)$  is not very stable: better is to have several such functions (provided that they do indeed have different relative amounts of ground state and excited state).

As an example of this discussion, I use some preliminary UKQCD data for the nucleon mass determination. With just one quantity measured (the local source - local sink: LL), a plateau in the effective mass was found as shown in fig 6. This shows a typical problem: the effective mass decreases out to large  $t$ -values. I have called this the ‘‘droop’’. It is difficult to be sure whether such a behaviour is statistically significant or not. For instance, a 2-exponential fit to the same data gives a significantly higher value of  $m_0$ . A resolution of this dichotomy comes from adding more measurements: SL and SS where S refers to a smeared source or sink. The combined fit to the 3 types of data is shown in fig 7 and strongly favours the 2-exponential fit with the higher  $m_0$  value.

#### 2.4.1. Correlations among data

It is widely known that, particularly for hadronic measurements, the data  $C_{ab}(t)$  are strongly correlated statistically. For example  $C_{ab}(t)$  and  $C_{ab}(t+1)$  are often 99% correlated. By this I mean that each fluctuates among lattice samples within its error, but that when the value at  $t$  is above average then so will be the value at  $t+1$ . This means that each  $t$  value is very far from statistically independent. The standard way to accommodate this is to use ‘correlated  $\chi^2$ ’.

The drawback of this method is that it can become unstable if the number of lattice samples  $N$  is insufficient when there are  $D$  types of data being fitted (ie  $D$  is number of  $t$ -values times number of types of measurement). The expected  $\chi^2$  per degree of freedom from such a correlated  $\chi^2$  fit is [21]

$$\frac{\chi^2}{\text{d.o.f.}} = 1 + \frac{D+1}{N} + \mathcal{O}(N^{-2}) \quad (7)$$

Moreover, if  $D \geq N$ , then  $\chi^2$  becomes infinite since the correlation matrix among the data is non-invertible.

This is a problem in practice: if 15  $t$ -values are to be fitted with 3 types of observable then  $D = 45$  while  $N$  is typically between 50 and 200. The recommended way forward is to parametrise the correlations among the data with fewer parameters than the general case (which has  $D(D-1)/2$ ). This should ensure a stable evaluation of the inverse of the correlation matrix and, in particular, avoid the problem of spurious small eigenvalues of the sample correlation matrix. Various suggestions have been made to accomplish this: an SVD inverse [22], 3 and 5-diagonal inverses [23], averaging of small eigenvalues of the correlation matrix [23], etc. The methods used will need to take into account the nature of the correlations among the data in each application and then model them in a stable way [23]. A program incorporating a broad selection of these methods is available from the author.

The alternative to such modelling of correlations is to have enough independent data samples  $N$ . Data sets containing of the order of thousands of configurations analysed are going to be needed for precision hadron spectroscopy on a lattice.

#### 2.4.2. Efficient hadronic operators

The strategy for fitting the data to extract mass values involves using several hadronic operators. For example local and smeared operators were used in the previous illustration. The availability of several operators allows a variationally improved operator to be constructed for the ground state. It is, never the less, necessary to select such an operator basis wisely.

It is important to explore this choice of oper-

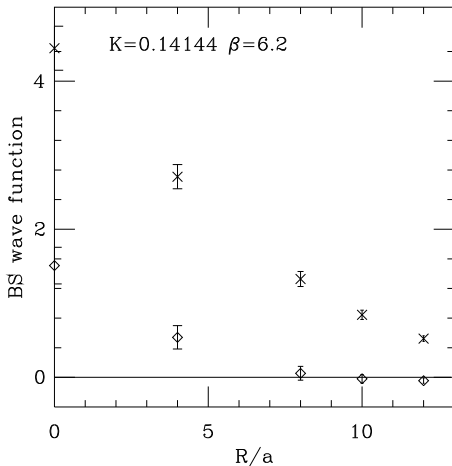


Figure 8. The Bethe Saltpeter wave function for the  $\rho$  and  $\rho'$  from ref [27]

ators to find efficient ones. The definition of efficient in this context is that the contribution of excited states is minimised relative to the ground state contribution. Non-local operators modelled on heavy quark bound states are promising candidates: they would be the optimum choice in the limit of heavy quarks and so may still be appropriate for lighter quarks. The construction used is to join the quark and anti-quark in a meson by a straight colour flux path of length  $R$ . Following experience of potential studies [24], this flux path is made from smeared links. The resulting overlap amplitude  $\langle 0|q(0)U(0 \rightarrow R)\Gamma_M\bar{q}(R)|M \rangle$  is often referred to as the Bethe-Saltpeter amplitude of meson  $M$  (where  $\Gamma_M$  is  $\gamma_i$  for the  $\rho$ , etc). This has been studied before [26,25] to learn about the spatial distribution of hadrons. The new observation [27] is that the same quantity for the first excited state (eg.  $\rho'$ ) has a node. Thus choosing the separation  $R$  at this node will give an efficient operator to make the ground state with no contamination from that first excited state. As illustrated in fig 8, this node is at  $R \approx 3 \text{ GeV}^{-1}$ . Results for baryons are also qualitatively similar [27].

### 3. THE QCD RUNNING COUPLING

The world average of the QCD running coupling compiled by Webber [28] is

$$\alpha_{\overline{\text{MS}}}^{(5)}(M_Z) = 0.117(5).$$

This average includes input from lattice analyses. Indeed the lattice determinations have the smallest errors quoted. Since the precise value of  $\alpha_S$  is important for phenomenology and for attempts to look for evidence of models beyond the standard model, it is important for the lattice community to understand fully the source of errors in the lattice determinations. This is highlighted by the change from the value 0.108(6) quoted [29] at Lattice 1993 to a value of 0.115(2) quoted [30] this year.

There are two requirements to measure  $\alpha_S$  on a lattice:

- (i) an accurate match to perturbation theory
- (ii) an accurate lattice energy scale set by some experimental input (eg.  $m_\rho$ ,  $V(R)$ , 1P-1S heavy onia, etc)

#### 3.1. Perturbation theory on a lattice

First I discuss the requirement that perturbation theory is accurately reproduced on the lattice so that  $\alpha_S$  can be defined. Consider first perturbation theory in terms of the bare lattice coupling  $g^2 = 6/\beta$  with  $\alpha = g^2/4\pi$ . The plaquette action  $S_\square$  has been calculated [31] for  $N_f = 0$  to order  $\alpha^3$  for the Wilson gauge action. For SU(3) colour,

$$\begin{aligned} \alpha_\square &\equiv -\frac{3}{4\pi} \log(S_\square) \\ &= \alpha(1 + 3.37\alpha + 17.69\alpha^2 + \dots) \end{aligned} \quad (8)$$

Now at  $\beta = 6.5$ ,  $\alpha = 0.07346$  and the last expression evaluates to 92% of the first expression obtained from the measured lattice plaquette action. The  $\alpha^3$  term contributes 7%. So we do not have a good convergence of perturbation theory. Increasing  $\beta$  substantially to decrease  $\alpha$  is not feasible with present computing techniques.

The way forward has been known for a long time. A *physical definition* of  $\alpha$  should yield a perturbative series with coefficients which are much smaller than in the case of the bare coupling. Consider several such physical definitions:

- (i)  $\alpha_V$  from  $V(q)$  or  $S_\square$  [11].

(ii)  $\alpha_{q\bar{q}}$  from the force  $dV/dR$  [32].

(iii)  $\alpha_{SF}$  from the Schrödinger functional [33].

A variant of  $\alpha_{SF}$  with twisted boundary conditions has recently been used [34].

Consider the first case, where the Fourier transform of the static potential is used as a definition:  $3q^2V(q) = -16\pi\alpha_V(q)$ . Then the logarithm of the plaquette action can be re-expressed in terms of this definition:

$$\alpha_{\square} = \alpha_V(1 - (1.19 + 0.07N_f)\alpha_V + \mathcal{O}(\alpha_V^2)) \quad (9)$$

where  $\alpha_V$  has scale  $q = 3.41/a$  [11]. Indeed the coefficient of  $\alpha^2$  is now  $\mathcal{O}(1)$ . The expectation is that all coefficients in such an expansion are  $\mathcal{O}(1)$ . For our present purposes it is the coefficient of the  $\alpha_V^3$  term above that is assumed to be  $\mathcal{O}(1)$ .

This coefficient can be obtained by evaluating the perturbative connection between the bare and  $V$ -scheme coupling to order  $\alpha^3$  since the link between  $S_{\square}$  and bare coupling is known (though only for  $N_f = 0$ ). Indeed, since the calculation of the connection between  $\alpha_{\overline{\text{MS}}}$  and the bare coupling is under way [36], it will soon be possible to determine  $\alpha_{\overline{\text{MS}}}$  directly from  $S_{\square}$  to relative accuracy of  $\mathcal{O}(\alpha^3)$ . Meanwhile, the connection of the  $\overline{\text{MS}}$  and  $V$  schemes is only known to lower order. For example for  $\text{SU}(3)$  of colour,

$$\alpha_{\overline{\text{MS}}} = \alpha_V(1 - (0.822 - 0.088N_f)\alpha_V + \mathcal{O}(\alpha_V^2))(10)$$

When comparing  $\alpha$  in different schemes, the scales in the two schemes can in principle be chosen differently. Possible choices are to take them equal, choose them so that the  $\mathcal{O}(\alpha^2)$  term is exactly zero, or some compromise. From a comparison of the Schrödinger Functional and Twisted Polyakov methods in  $\text{SU}(2)$ , there is a definite preference [35] for the prescription of choosing the relative scale (as the ratio of  $\Lambda$  parameters) so that the  $\mathcal{O}(\alpha^2)$  term is exactly zero. As a further example of this ambiguity, eq 10 can be expressed [30] as

$$\alpha_{\overline{\text{MS}}}(q) = \alpha_V(e^{5/6}q)(1 + 0.637\alpha_V + \mathcal{O}(\alpha_V^2)) \quad (11)$$

The difference between these expressions is  $\mathcal{O}(\alpha^3)$  and so a preference can only be made when the  $\alpha^3$  calculation is completed.

Until the  $\alpha^3$  calculations are completed, some cross checks are worth making. One approach [37]

is to use Monte Carlo evaluation on lattices with a wide range of  $\beta$  to estimate the size of the  $\alpha_V^3$  correction in eq. (9). The method is to compare the extraction of  $\alpha_V$  from  $1 \times 1$ ,  $1 \times 2$ ,  $1 \times 3$  and  $2 \times 2$  Wilson loops. Then, relative to the (unknown) coefficient of the  $1 \times 1$  extraction, the other cases have  $\alpha^3$  coefficients of 0.36, 0.53 and 0.97 respectively. This is indeed confirmation that coefficients  $\mathcal{O}(1)$  are plausible.

Another cross check is to use the recent perturbative evaluation [38] of  $\alpha_{SF}$  in terms of the bare coupling to obtain for  $\text{SU}(2)$  of colour:

$$\alpha_{\square} = \alpha_{SF}(1 - 0.737\alpha_{SF} + 0.039\alpha_{SF}^2 + \dots) \quad (12)$$

with scale  $a = q^{-1} = L$ . This is the first relationship to be obtained to this order between two physically defined lattice couplings. The coefficients are indeed less than one, although with the caveat that  $\text{SU}(2)$  colour tends to have smaller coefficients than  $\text{SU}(3)$ .

Besides evaluating  $\alpha_V$  from  $S_{\square}$ , it can be directly obtained from the static quark potential [39]. Present results are compatible between the two methods within the inherent errors of each.

Many phenomenological models have been proposed to obtain an improved definition of  $\alpha$  in lattice studies [40–42] by modifying the bare coupling. These suggestions were constructed with the intention of rendering the perturbative coefficients of  $\mathcal{O}(1)$ . In this respect they are similar to the  $\alpha_V$  scheme outlined above but, because they are empirical in origin, they are less appropriate to a precision analysis of  $\alpha$ .

Since  $S_{\square}$  is the shortest distance quantity defined on a lattice, it corresponds to the highest momentum. It is also easy to measure accurately. Thus it is a very popular starting point for extracting  $\alpha$ . Indeed,  $\alpha_{\overline{\text{MS}}}$  can be obtained from the measured  $S_{\square}$  with error  $\mathcal{O}(\alpha^3)$ . In order to check that perturbation theory is accurate, the coefficient of this  $\alpha^3$  term should be evaluated (this is in progress) and then the values of  $\alpha_{\overline{\text{MS}}}$  from different lattice spacings should be compared with the perturbative evolution through the beta-function. If this perturbative evolution were accurate above some scale  $q = 1/a$ , then one would have confidence in this method of ex-

tracting  $\alpha$ . For the other methods of defining and extracting  $\alpha$ , the same checks are needed and they have been thoroughly explored for the Schrödinger Functional scheme in the quenched approximation [33]. This check of the evolution is essential to control possible non-perturbative effects which I now discuss.

### 3.2. Non-perturbative contributions

Since the method employed is to extract  $\alpha$  from lattice measurements, there may be a non-perturbative component present in principle. Note that such non-perturbative components are also equally important in continuum/experimental determinations of  $\alpha_S$ . I shall illustrate this problem by considering the “force” definition of the coupling. For SU(3) colour with  $N_f = 0$ , this is

$$\alpha_{q\bar{q}}(q) = \frac{3}{4}R^2 \frac{dV}{dR} \text{ with } q = \frac{1}{R} \quad (13)$$

Now, since the force  $dV/dR$  has a non-perturbative contribution from the string tension  $K$ , one could equally well introduce a modified definition by subtracting it:  $\tilde{\alpha} = \alpha_{q\bar{q}} - 3KR^2/4$ . Since  $\alpha \approx b_0/\log(R^{-2})$ , the two definitions of  $\alpha$  differ by a term proportional to  $\exp(-b_0/\alpha)$ . This is a non-perturbative difference: the two definitions agree to all orders of perturbation theory. For  $q = R^{-1} \gg 10$  GeV, this non-perturbative piece is negligible ( $< 1\%$ ). However, one should keep in mind that different “physical” definitions of  $\alpha$  could have different non-perturbative components. For example when extracting  $\alpha_V$  from  $S_\square$ , the typical momentum scale is large ( $q^* = 3.4/a$ ) but it arises from a cancellation of  $q_i = 0$  and  $q_i = \pm\pi/a$ . So non-perturbative effects could arise even though  $q^* > 10$  GeV.

### 3.3. Comparison of $\alpha_S$ determinations

I now make a comparison of several methods of extracting  $\alpha_{\overline{\text{MS}}}$  from lattice measurements. To make the comparison as close as possible, the scale is set in each case from the best measured quantity (the static quark potential at moderate interquark separations) with the definition  $r_0^2 dV/dR|_{r_0} = 1.65$ . This definition [43] corresponds to  $r_0 \approx 0.5$  fm and to  $\sqrt{K}r_0 \approx 1.2$ . To

have the most accurate lattice data, I use the quenched determinations for SU(3) colour.

(i) Then at  $q = 37/r_0$  (approx 15 GeV), the Schrödinger functional method obtains [33]

$$\alpha_{\overline{\text{MS}}} = 0.1108(23)(10)$$

where the first error is from the scale and the second is assuming the  $\alpha^3$  correction has coefficient  $\pm 1$ .

(ii) The method of extracting the coupling from the plaquette action  $S_\square$  (via  $\alpha_V$ ) yields

$$\alpha_{\overline{\text{MS}}} = 0.1151(5)(13)$$

where data [46] at  $\beta = 6.5$  has been used which corresponds to  $q^* = 38.3/r_0$  and this has been run to  $37/r_0$  using 2-loop formulae.

(iii) The last method uses the force and, at the highest  $\beta$ -values currently available [46] of 6.5, corresponds to  $q < 7/r_0$  only. However, it gives results for a range of  $q$ -values consistent with two-loop running. Assuming two-loop running to  $37/r_0$ , then yields

$$\alpha_{\overline{\text{MS}}} = 0.1180(21)(13) \left( \begin{smallmatrix} +0 \\ -60 \end{smallmatrix} \right)$$

where the last error term comes from the possible non-perturbative effect of removing the string tension before running the coupling. There is no sign in the data for any such non-perturbative effect but its absence can only be confirmed by going to smaller lattice spacing.

These values are in reasonable agreement with each other. The  $\mathcal{O}(\alpha^3)$  terms need to be calculated to refine the comparison further (this will remove the 1% error from assuming the coefficients are within  $\pm 1$ ). A guide to the possible size of the  $\mathcal{O}(\alpha^3)$  terms comes from comparing the different definitions of  $\alpha$  at different scales so that the  $\alpha^2$  terms vanish - rather than at the same scale. Some evidence exists [34,38,35] that this prescription works well for SU(2). For the Schrödinger functional method, this would then yield

$$\alpha_{\overline{\text{MS}}} = 0.1141(24)(15)$$

The difference from the result quoted above is approximately  $2.5\alpha^3$  which shows that coefficients of that magnitude are plausible in this case. Moreover, this scale choice gives a value in closer agreement with the other methods.

After this perturbative calculation, any remaining difference in  $\alpha$  values must be ascribed to non-perturbative effects. Since any non-

perturbative effects are rather different in the first method (which involves the small-volume vacuum) than in the latter two determinations, this will be a valuable cross check.

This comparison highlights that caution is needed in extracting  $\alpha$  from lattice data. Consistency as the momentum scale is increased is essential.

### 3.4. Setting the Scale

The requirement is that dimensionless ratios of physical quantities are independent of the lattice spacing  $a$  so that the scale can be set unambiguously. Because of uncertainties in corrections due to quenching and to  $\mathcal{O}(a)$  effects, there is still a measure of uncertainty in setting the scale.

The most accurate lattice measurement is indeed  $r_0$  from the static potential  $V(R)$  as discussed above. This definition, unlike that in terms of the string tension, is also applicable to full QCD. Indeed this is the method of choice for comparisons between different lattice evaluations. Of course,  $r_0$  is not directly known experimentally, so other quantities are also used.

The  $\rho$  mass is often chosen although the extrapolation of  $m_q \rightarrow 0$  (or the physical light quark masses) introduces errors. The effect of incomplete treatment of the decay  $\rho \rightarrow \pi + \pi$  is most probably quite small on the  $\rho$  mass.

Another choice is  $f_\pi$  but the renormalisation factor  $Z_A$  then needs to be evaluated. This needs an accurate perturbative evaluation - cross checked by non-perturbative methods - see the review by Martinelli [47].

A very popular choice is the 1P-1S mass splitting in heavy onia. This choice is supported by two encouraging indications: (i) empirically, the mass splitting depends very little on the heavy quark mass and (ii) the relevant momenta (for instance as indicated by the wave function) are expected not to be so sensitive to very light quark effects. The drawback is that for relativistic fermions  $m_c a$  is comparable to 1, so  $\mathcal{O}(a)$  effects are potentially large. This can be avoided by using an effective lagrangian appropriate to heavy quarks for the  $b\bar{b}$  system: for example a non-relativistic treatment. This requires a careful calibration of the effective lagrangian. The

NRQCD method, see ref [10], involves an effective lagrangian which can be refined in principle by evaluating more terms. The inherent errors are not straightforward to estimate.

For the quenched approximation, the (1P-1S)/(2S-1S) ratio for  $b\bar{b}$  comes out [30] from NRQCD as 0.71 (similar to the static potential value [24]) which differs from the experimental value of 0.78. This can induce some uncertainty in setting the scale.

The running of the coupling reduces the dependence on the scale as the momentum is increased:  $\Delta\alpha/\alpha \approx 0.2 \Delta q_0/q_0$  at  $q = M_Z$ . Thus a 10% error in the scale  $q_0$  results in a relative error of 2% on  $\alpha$  at  $M_Z$ .

### 3.5. $\alpha_S$ from dynamical quark simulations

Until recently, attempts to evaluate  $\alpha_S$  from lattices used quenched simulation and corrected for the effects of quenching via a phenomenological potential approach [29]. This certainly captured one of the main corrections to quenching: namely the stronger interquark force at small separation (by a factor of  $33/(33 - 2N_f)$ ). However, corrections at moderate and large separations were treated empirically. This year, several groups have used dynamical quark simulations directly. These have mainly involved 2 flavours of staggered quarks and the coupling has been determined by relating  $\alpha_{\overline{\text{MS}}}$  to the plaquette action by perturbation theory. For example [30], the plaquette action gives  $\alpha_V(3.41/a) = 0.1785(56)$  at  $\beta = 5.6$  for 2 flavours of staggered quarks with  $ma = 0.01$ . Here the error comes from assuming the  $\alpha^3$  coefficient is  $\pm 1$ . The scale has been set by either  $m_\rho$  or the 1P-1S splitting in onia. After processing the  $N_f = 0$  and  $N_f = 2$  results to obtain  $N_f = 3$ , in each case the result obtained for 3 light flavours at moderate  $q$  has been run to  $q = M_Z$  in the conventional way to facilitate comparisons.

Using Wilson valence quarks, the result [44] obtained is

$$\alpha_{\overline{\text{MS}}}(M_Z) = 0.111(5)$$

where an extrapolation of  $S_\square$  to  $m_q = 0$  has been made. The result for  $N_f = 2$  has been corrected to  $N_f = 3$  by using 2-loop running down to  $\approx 0.5$  GeV with 2 flavours and then back up

with three. The authors compare the quenched and unquenched  $\alpha$  values and find that they overlap at low  $q$  values. This is some support for their method of correcting to  $N_f = 3$  (and incidentally for the method used to go directly from  $N_f = 0$  to  $N_f = 3$  [29]). A similar approach using staggered valence quarks [45] shows sizable flavour breaking effects, particularly for heavier quarks, and thus relatively large systematic errors.

Another group [30] has used NRQCD to evaluate the  $b\bar{b}$  spectrum with dynamical quark configurations. They extrapolate  $\alpha^{-1}$  in  $N_f$  from  $N_f = 0$  and 2 to get to  $N_f = 3$ . Using a fixed dynamical quark mass  $am_q = 0.01$  at  $\beta = 5.6$ , gives

$$\alpha_{\overline{\text{MS}}}(M_Z) = 0.115(2)$$

A preliminary result has been obtained [48] using the same configurations but with Wilson valence fermions. The main difference comes from the lattice scale as  $a^{-1} = 1.9$  GeV rather than 2.4 GeV as found from NRQCD. Their result is

$$\alpha_{\overline{\text{MS}}}(M_Z) = 0.108(6)$$

Note also that using  $r_0$  to set the scale on the same configurations [15] yields  $r_0/a = 5.2(3)$  which gives  $a^{-1} \approx 2.0$  GeV. This agrees with the Wilson valence result but differs from the NRQCD value from the same configurations. The NRQCD value relies on perturbative evaluation of coefficients in the lagrangian, so non-perturbative corrections introduce an error which is hard to quantify. The direct full QCD determinations have scale errors of  $\mathcal{O}(a)$  which can be reduced by increasing  $\beta$ .

In view of the uncertainties of order 4% found in the quenched case with much smaller lattice spacings, it seems prudent to include errors at least of this size to allow for possible non-perturbative effects and possible effects from the unknown perturbative coefficients at  $\mathcal{O}(\alpha^3)$ . Further, the scale error is presently some 20% which implies a 4% error in  $\alpha(M_Z)$ . In summary, I propose that at least a 6% error should be ascribed to the lattice results. Even so, a reasonable average of current lattice determinations would yield 0.112(7). This is still of significance since the world average quoted above was 0.117(5).

To improve on this, calculations at increased  $\beta$  are needed to explore non-perturbative effects

and  $\mathcal{O}(a)$  effects. Further variation of  $m_q$  and  $N_f$  should be explored. The  $\mathcal{O}(\alpha^3)$  terms in the perturbative matching also need to be evaluated. Several of these steps are under way and it should soon be possible to evaluate  $\alpha_{\overline{\text{MS}}}$  at  $q \approx 10$  GeV to high accuracy from lattice studies. Assuming the conventional 3-loop evolution from 10 GeV, this will yield  $\alpha(M_Z)$  to 1%.

#### 4. THE INTERACTION BETWEEN COLOUR SOURCES

As well as explicit study of the spectrum and coupling of hadrons, it is instructive to look at qualitative features of QCD. The confining mechanism is the clearest example. One consequence of confinement is that the potential energy  $V(R)$  between static colour sources in the fundamental representation grows with increasing separation  $R$ . In the quenched approximation, this potential continues to grow approximately linearly for large  $R$  - as  $KR$  where  $K$  is the string tension. The name string tension comes from the observation that a string theory can yield such a behaviour. To study this confining force in more detail, there are several topics to pursue: a detailed measurement of  $V(R)$  at large  $R$  is of interest; the spatial distribution of the energy in the colour flux can be determined; the spin dependence of the long range force can be explored. These topics have been of interest for many years. Increased computational resources have enabled major increases in precision recently. Because it is qualitative features that are to be explored, it is sufficient to use SU(2) colour for initial investigations. This allows considerable increase in precision since it is computationally faster.

As well as studying the strong force between two heavy quarks, it is of interest to explore the much weaker forces between hadrons. These can be studied by looking at 4 quark potentials in SU(2).

##### 4.1. The self-energy of the hadronic string

The self-energy of closed string-like flux tubes of length  $L$  (called torelons) has been studied in SU(2) gauge theory [49]. For  $L > 1$  fm, the energy of such torelons was found to have a compo-

ment  $f\pi/3L$  with  $f = 1.00(3)$ , exactly the coefficient expected from string fluctuations. This is a test of the zero point fluctuations of a string. The string excitations themselves give rise to excited states of the potential between static sources and they have been found previously [13] to agree well.

#### 4.2. The colour flux tube

The Wuppertal group [50] have explored the spatial distribution of the colour fields between static quarks in SU(2) with separations out to  $R \approx 2$  fm. At smaller  $R$ , their results are similar to features seen previously [51]. The question of interest is the transverse profile of the colour flux tube. They find that the width of this transverse flux profile increases quite fast with  $R$  until  $R \approx 1$  fm when the increase levels off. By looking at the differences in the distribution of colour flux as  $R$  is increased, they find consistency with the picture that a string-like configuration exists for  $R \geq 0.75$  fm. The data are shown in fig 9 and are consistent with the expected increase of the width as  $\log R$  in this region, but the evidence is not compelling. The breakdown into colour magnetic and colour electric contributions is measured and this is a constraint on phenomenological models of the confining flux tube.

#### 4.3. The spin dependent force

From earlier work, we know that the force between static quarks has a short ranged component roughly like one gluon exchange and a long range component which is dominantly in the  $V_1'$  rather than  $V_2'$  spin-orbit term (this corresponds to Lorenz ‘scalar’ confinement in the usual description). In order to get more precision, it is necessary to go to smaller lattice spacing to study the spin dependent potentials since they vary very rapidly at small  $R$ .

Recent work [52] confirms the earlier qualitative results and shows some evidence for small but significant departures from the simple picture of one gluon exchange together with a string component. The region studied is  $R \leq 0.3$  fm. In this  $R$  region, the new results confirm that the confining component is dominantly in  $V_1'$ . As well as this string tension term  $K$  in  $V_1'(R)$ , there is also evidence for an additional attractive  $1/R^2$  piece.

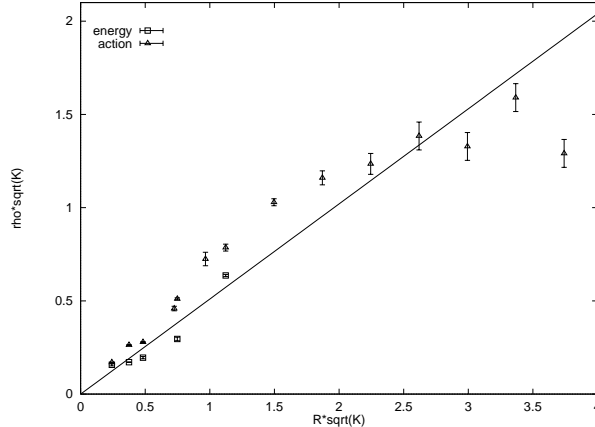


Figure 9. The half width  $\rho$  of the energy and action flux tube at source separation  $R$  in units of the string tension  $K$ .

Since 1 gluon exchange does not contribute to  $V_1'$ , such a component could arise from the string fluctuation term ( $-\pi/12R$  in  $V_0(R)$ ) or from multiple gluon exchange.

A careful theoretical study of the nature of the spin-orbit force to be associated with the long range string fluctuation component would be very useful since some relevant lattice data now exists.

#### 4.4. The force between hadrons

The colour force between static fundamental-representation quarks is far stronger than the residual ‘strong’ force between hadrons. It has always been difficult to explore this ‘strong’ force in lattice simulation because the binding energy is so much smaller than that from the colour force. For example for SU(2) of colour and for 2 quarks and 2 antiquarks, the difference  $V_4 - 2V_2$  between the 4-body potential and that of the two pairs taken separately is typically much less than 1% of  $2V_2$ . Nevertheless, results have been obtained for the binding energy for a number of different geometrical arrangements of the 4 static sources [53]. The value of the observed binding energy can be understood qualitatively from mixing between dif-

ferent pairings of the two body potentials. One strong conclusion from this study [53] is that the four body system is *not* well approximated as a sum of two body components.

## 5. CONCLUSIONS

Often the progress in a field is hard to see year by year. New ideas become accepted gradually and less accurate methods wither gently. The progress is often that problems are no longer discussed, since new methods have circumvented the obstacle.

One area of progress has been in understanding the best way to study the QCD coupling on a lattice. The agreement between different methods gives confidence. Present estimates correspond to a value  $\alpha_{\overline{\text{MS}}}(M_Z) = 0.112(7)$  and a clear route exists to reduce this error to about 1%.

Quenched QCD is currently in good shape. The sources of error are understood and steps are being taken to reduce them. Accurate spectral results in the quenched approximation are of importance, both because they enable us to understand QCD better and because they provide a calibration for calculations of matrix elements, etc. The full QCD program is less advanced because of computational limitations. Studies so far have used rather small lattices, rather coarse lattice spacing, and rather heavy quarks. With future increases in computer power and future improvements in algorithms, it will be possible to explore full QCD as thoroughly as the quenched approximation is currently studied.

## REFERENCES

1. D. Chen, these proceedings.
2. APE Collaboration, S. Antonelli et al., hep-lat 9405012 and these proceedings, hep-lat 9411083.
3. F. Butler et al., hep-lat 9405003; Nucl. Phys. B421 (1994) 217.
4. T. Battacharya, R. Gupta and J. Grandy, these proceedings.
5. S. Gottlieb, these proceedings, hep-lat 9412021.
6. B. Sheikholeslami and R. Wohlert, Nucl. Phys. B259 (1985) 572; G. Heatlie et al., Nucl. Phys. B352 (1991) 266.
7. UKQCD Collaboration, C. R. Allton et al., Phys. Rev. D 49 (1994) 474.
8. APE Collaboration, C. R. Allton et al., Phys. Lett. B326 (1994) 295; Nucl. Phys. B413 (1994) 461.
9. R. Sommer, these proceedings.
10. J. Sloan, these proceedings.
11. G. P. Lepage and P. B. Mackenzie, Phys. Rev. D48 (1993) 2250.
12. A. Hasenfratz, these proceedings.
13. C. Michael, Nucl. Phys. B (Proc. Suppl.) 16 (1990) 559.
14. S. Aoki et al., Phys. Rev. D50 (1994) 486.
15. U. M. Heller et al., hep-lat 9401025.
16. R. Gupta, these proceedings.
17. UKQCD Collaboration, G. Bali et al., Phys. Lett. B309 (1993) 378.
18. H. Chen et al., Nucl. Phys. B (Proc. Suppl.) 34 (1994) 357.
19. J. Sexton, A. Vaccarino and D. Weingarten, these proceedings.
20. Y. Kuramashi et al., Phys. Rev. Lett. 72 (1994) 3448.
21. C. Michael, Phys. Rev. D49 (1994) 2616.
22. I. T. Drummond and R. R. Horgan, Phys. Lett. B302 (1993) 271; G. Kilcup, Nucl. Phys. B (Proc. Suppl.) 34 (1994) 350.
23. C. Michael and A. McKerrell, Liverpool preprint LTH 342.
24. S. J. Perantonis and C. Michael, Nucl. Phys. B347 (1990) 854.
25. K. B. Teo and J. W. Negele, Nucl. Phys. B (Proc. Suppl.) 34 (1994) 390.
26. R. Gupta, D. Daniel and J. Grandy, Phys. Rev. D48 (1994) 3330.
27. UKQCD Collaboration, presented P. Lacock, these proceedings, hep-lat 9411013.
28. B. R. Webber, Proc. Int. Conf. HEP, Glasgow 1994, Cavendish preprint HEP 94/15.
29. A. X. El-Khadra, Nucl. Phys. B (Proc. Suppl.) 34 (1994) 141.
30. C. T. H. Davies et al., hep-ph 9408328; see also J. Sloan, these proceedings.
31. B. Alles et al., Phys. Lett B324 (1994) 433.
32. C. Michael, Phys. Lett. B283 (1992) 103.
33. M. Lüscher et al., Nucl. Phys. B359 (1991) 221;

- Nucl. Phys. B413 (1994) 481.
34. G. de Divitiis et al., Nucl. Phys. B (in press), hep-lat 9407028.
  35. G. de Divitiis et al., hep-lat 9411017 and M. Guagnelli, these proceedings, hep-lat 9411035.
  36. M. Lüscher, A. van de Ven and P. Weisz, these proceedings.
  37. W. Dimm et al., (in preparation) quoted in ref [30].
  38. R. Narayanan and U. Wolff, these proceedings, hep-lat 9411018.
  39. T. R. Klassen, hep-lat 9408016 and these proceedings, hep-lat 9412022.
  40. G. Parisi in Proc. XX Int. Conf, AIP (1981), (eds. L. Durand and L. G. Pondrom).
  41. F. Karsch and R. Petronzio, Phys. Lett. 139B (1984) 403.
  42. The mean field improved prescription in ref[11].
  43. R. Sommer, Nucl. Phys. B411 (1994) 839.
  44. S. Aoki et al., hep-lat 9407015.
  45. S. Aoki et al., these proceedings, hep-lat 9411058.
  46. UKQCD Collaboration, S. P. Booth et al., Phys. Lett. B294 (1992) 385.
  47. G. Martinelli, these proceedings.
  48. M. Wingate et al., these proceedings, hep-lat 9411041.
  49. C. Michael and P. W. Stephenson, Phys. Rev. D50 (1994) 4634.
  50. G. S. Bali, K. Schilling and C. Schlichter, hep-lat 9409005 and these proceedings, hep-lat 9412018.
  51. R. W. Haymaker, V. Singh and Y. Peng, hep-lat 9406021
  52. G. S. Bali, K. Schilling and A. Wachter, these proceedings, hep-lat 9412002.
  53. A. M. Green et al., these proceedings, and references contained therein.